Science of the Total Environment 640-641C (2018) 1098–1111

Contents lists available at ScienceDirect

Science of the Total Environment

journal homepage: www.elsevier.com/locate/scitotenv

Wind-driven rain and future risk to built heritage in the United Kingdom: Novel metrics for characterising rain spells

Scott Allan Orr[a,b,*], Maureen Young[c], Dawson Stelfox[d], Joanne Curran[d], Heather Viles[a]

[a] School of Geography and the Environment, University of Oxford, South Parks Road, Oxford OX1 3QY, United Kingdom
[b] EPSRC CDT in Science and Engineering in Arts, Heritage, and Archaeology, 14 Upper Woburn Place, London WC1H 0NN, United Kingdom
[c] Historic Environment Scotland, The Engine Shed, Stirling, Forthside Way, Stirling FK8 1QZ, United Kingdom
[d] Consarc Design Group, The Gas Office, 4 Cromac Quay, Ormeau Road, Belfast BT7 2JD, United Kingdom

HIGHLIGHTS

- Semi-empirical assessment of exposure to wind-driven rain for 8 UK sites
- Late 21st century conditions evaluated by probabilistic generation of hourly weather
- Future exposure predicted to become more polarised in winter and summer months
- Rain spells predicted to be shorter but have more intense and concentrated exposure
- Increased runoff, biological growths, moisture cycling and deep-seated wetting

GRAPHICAL ABSTRACT

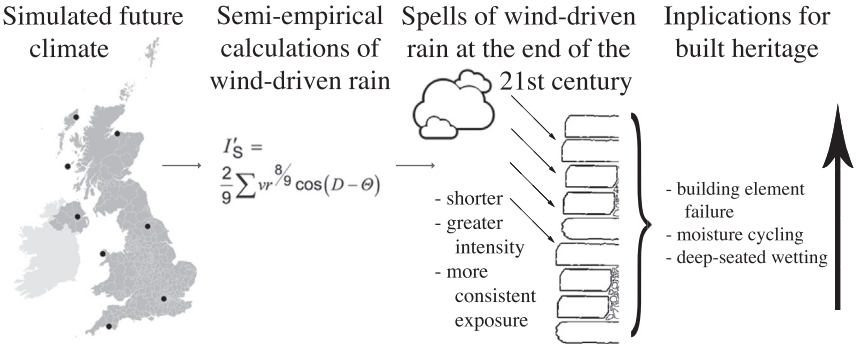

ARTICLE INFO

Article history:
Received 9 March 2018
Received in revised form 4 May 2018
Accepted 24 May 2018
Available online 6 June 2018

Editor: R Ludwig

Keywords:
Climate change
Heritage conservation
Risk assessment
Building performance
building moisture
Sustainability

ABSTRACT

Wind-driven rain (WDR) is rain given a horizontal velocity component by wind and falling obliquely. It is a prominent environmental risk to built heritage, as it contributes to the damage of porous building materials and building element failure. While predicted climate trends are well-established, how they will specifically manifest in future WDR is uncertain. This paper combines UKCP09 Weather Generator predictions with a probabilistic process to create hourly time series of climate parameters under a high-emissions scenario for 2070–2099 at eight UK sites. Exposure to WDR at these sites for baseline and future periods is calculated from semi-empirical models based on long-term hourly meteorological data using ISO 15927-3:2009. Towards the end of the twenty-first century, it is predicted that rain spells will have higher volumes, i.e. a higher quantity of water will impact façades, across all 8 sites. Although the average number of spells is predicted to remain constant, they will be shorter with longer of periods of time between them and more intense with wind-driven rain occurring for a greater proportion of hours within them. It is likely that in this scenario building element failure – such as moisture ingress through cracks and gutter over-spill – will occur more frequently. There will be higher rates of moisture cycling and enhanced deep-seated wetting. These predicted changes require new metrics for wind-driven rain to be developed, so that future impacts can be managed effectively and efficiently.

* Corresponding author at: School of Geography and the Environment, University of Oxford, South Parks Road, Oxford OX1 3QY, United Kingdom.
E-mail address: scott.orr@ouce.ox.ac.uk (S.A. Orr).

https://doi.org/10.1016/j.scitotenv.2018.05.354

1. Introduction

The IPCC was virtually certain[1] in 2013 that the troposphere has warmed since the mid-20th century and had high confidence[2] that global precipitation patterns have changed – trends that are likely to continue over the twenty-first century (IPCC, 2013). These changes pose threats to natural and built heritage (Cassar, 2005), especially in the United Kingdom where more intense and frequent precipitation events are very likely.[3]

The presence and movement of water contributes to the weathering and deterioration of porous materials and other aspects of building performance. Traditional building materials such as stone and mortar, as well as concrete, are affected by many weathering processes in which water is implicated, such as chemical weathering (Charola and Ware, 2002), freeze-thaw weathering (Hall, 1999), salt weathering (Doehne, 2002) and biological weathering (Crispim and Gaylarde, 2005; Warscheid and Braams, 2000).

Wind-driven rain (WDR) or driving rain is rain given a horizontal velocity component by the wind and falling obliquely (Blocken and Carmeliet, 2004). WDR represents the main moisture source and cause of deterioration on most building façades (Erkal et al., 2012), as it is implicated in both long-term deep-set wetting (McCabe et al., 2013; Smith et al., 2011) and short-term risks of building element failure (e.g. rain penetration through edges of doors or windows (ISO, 2009), and additionally junctions and gaps).

Wind-driven rain exposure can be assessed in many ways. To evaluate local and microscale conditions omni-directional gauges and wall-mounted pressure plates have been used since the 1930s (Lacy, 1951), more recently in combination with numerical simulations of computational fluid dynamics, e.g. Briggen et al. (2009) and Pettersson et al. (2016). To determine regional characteristics, semi-empirical models of WDR have been developed. These are indices or relationships representing the volume of WDR exposure over a specific time period based on values of wind speed and direction and precipitation. As these variables are frequently measured by meteorological monitoring stations, WDR can be estimated for locations where this data is available. The aforementioned measurement, modelling, and semi-empirical techniques evaluate exposure to WDR. The susceptibility of building components to ingress can be assessed experimentally (e.g. BSI, 1970, 2001) or by using coupled heat and moisture transport differential equations models (e.g. WUFI Nik et al., 2015).

Wind-driven rain in the UK is expected to increase gradually over the twenty-first century, based on predicted increases of annual precipitation and days with intense rainfall (Brimblecombe, 2014; Holmes, 2015) under various emission scenarios. This raises doubt about the applicability and relevance to future conditions of current metrics and exposure maps to future conditions. In 2011 BRE Scotland advised that the present climate had not changed enough from the exposure reference maps published in 1992 (BSI, 1992) based on conditions in 1959–1991 to warrant an update (Reid and Garvin, 2011); practical experience suggests that changes in building performance during this century are already noticeable (Stelfox, 2018) compared to the twentieth century. While work has been done on site-level intervention techniques for increasing the resilience of traditional masonry (Laycock and Wood, 2014), little to date has evaluated how the characteristics of WDR might change during the twenty-first century.

The potential impact of climate change on cultural heritage is a growing academic concern (Fatorić and Seekamp, 2017), of interest for practical assessments undertaken at the site-specific level (Historic Environment Scotland, 2018). Using models or predictions is a crucial component of a robust moisture risk assessment, and should be considered as a tool for exploring possible risk (May and Sanders, 2017).

Semi-empirical evaluations of future WDR risk have been undertaken for Nordic regions including Sweden (Nik and Sasic Kalagasidis, 2014; Nik, 2017) and Finland (Pakkala et al., 2016). These studies have applied ISO 15927 or similar formulae (e.g. ASHRAE, 2009) to generated hourly data for future weather conditions. However, these studies have used 'morphing' (scaling) or unspecified processes to produce the future hourly time series (Nik, 2017 and Pakkala et al., 2016 respectively) which might not reflect the future temporal variation of WDR exposure. Nik and Sasic Kalagasidis (2014) have presented evaluations of future climate as annual means, which are generally more indicative annual variability and not of long-term climate changes. They have also presented a single future scenario, whereas the use of at least 100 different projected scenarios is advisable to robustly characterise future conditions. This type of analysis has not yet been undertaken for the UK, which will experience climate changes distinct from the aforementioned regions.

This paper assesses a predicted future scenario of wind-driven rain and risk to built heritage for eight locations in the UK in 2070–2099, based on generated time series of climate conditions from the UKCP09 weather generator (UK Climate Projections, 2012) and a probabilistic process of producing hourly time series (Eames et al., 2011a,b). The changing characteristics of wind-driven rain are assessed with standard indices and novel metrics based on additional attributes of wind-driven rain spells that emphasise temporal variability. A discussion of the implications of these changes for built heritage follows, considering building element failure, biological growth, near-surface cycling and deep-seated wetting.

2. Methods

2.1. Assessment technique selection

The main methods to assess the amount and intensity of wind-driven rain are measurements (Ge et al., 2017; Tang et al., 2004), semi-empirical models (ASHRAE, 2009; ISO, 2009; Straube and Burnett, 2000) and numerical methods (Choi, 1993); measurements are commonly used to verify the semi-empirical approaches and numerical simulations (Blocken and Carmeliet, 2007; Kubilay et al., 2015). Measurements and numerical methods – especially if the former incorporates computational fluid dynamics, e.g. Briggen et al. (2009) – can be costly, resource-intensive, and applied to a specific scenario of limited spatial scale. Semi-empirical models are based on climatic data from meteorological monitoring stations, and can incorporate the anthropogenic and natural context by applying factors, which are being continually improved (Ge et al., 2018). This facilitates comparisons between locations for which data is available, without requiring WDR-specific instrumentation at each site. Exposure maps based on semi-empirical models are commonly used in building assessment and design practice. For these reasons, a semi-empirical model was selected for this study.

2.2. The ISO model

ISO 15927 includes two driving rain indices that should be calculated from at least 10 years (and preferably 20 or 30) of continuous hourly data:

- **annual index I_A**: should be used for "considering the average moisture content of exposed building material or when assessing the likely growth of mosses and lichens" [BSI, 1992, p. 4]

[1] 99–100% probability.
[2] Defined as high agreement based on robust evidence.
[3] 90–100% probability.

- **spell index I_S**: " defined in terms of rain penetration through masonry, which requires a prolonged input of water"[ISO, 2009, p. 12]

It is important to note that neither of these directly reflects rain penetration through building elements (e.g. window frames, junctions, cracks, etc.…), which are dependent on short but intense WDR [ISO, 2009, p. v].

The volume of wind-driven rain that would hit a square metre in a 1 h period is calculated from[4]:

$$I = \frac{2}{9} v r^{8/9} \cos(D-\theta) \left[\mathrm{L\,m^{-2}}\right] \quad (1)$$

from average hourly wind speed v ($\mathrm{m\,s^{-1}}$), hourly precipitation r (mm), and hourly mean wind direction D° for a specific wall orientation θ°. These hourly exposures are used to calculate the indices in ISO 15927, and referred to as volumes hereafter.

The **annual index** I_A is calculated by the $\Sigma I/N$ for all hours in which $\cos(D-\theta) > 0$, i.e. when the wind is blowing against the wall; N is the number of years of data available. This is referred to as an *airfield* index in ISO 15927 as it represents WDR that would occur at a height of 10 m above ground level in the middle of an airfield with no other obstructions. According to ISO 15927, this is calculated as:

$$\mathrm{I}_A = \sum \frac{\frac{2}{9} v r^{8/9} \cos(D-\theta)}{N} \left[\mathrm{L\,m^{-2}}\right] \quad (2)$$

where the summation is taken over all the hours in which there is active WDR, i.e. $\cos(D-\theta) \geq 0$, and N is the number of years the summation is taken over.

A **spell-specific index** I_S' is calculated for an individual spell ΣI for all hours in which $\cos(D-\theta) > 0$ within that spell, also in $\mathrm{L\,m^{-2}}$. Spells are separated by periods of at least 96 h for which $v r^{8/9} \cos(D-\theta) \leqslant 0$, i.e. in which there is no WDR impacting a specific wall orientation. This is representative of airfield conditions, as described above for the annual index. See Fig. 1 for an example of a rain spell, as defined in ISO 15927. Experimental work by Caton at the UK Meteorological Office showed that up to 96 consecutive hours with no driving rain are necessary before evaporative losses will exceed water ingress from rain exposure (Prior, 1985); 96 h is also sufficient to bridge the gap between succeeding depressions in a weather sequence in the UK (Prior, 1983). In contrast to current standards, Caton distinguished between spells using periods of ⩾96 h without 'appreciable' driving rain, for which an approximate value of one tenth of the expected index for a once in three year spell for each orientation (Prior, 1985). 96 h is arguably an arbitrary delimiter between spells. It does not imply that 96 h is sufficient for all moisture ingress to exit the building envelope.

The **spell index** I_S is defined as the 66th percentile of all spells' I_S' in ISO 15927. Using percentiles to represent extreme events is dependent on their frequency of occurrence. Instead this was calculated from an Annual Maxima Series approach using 'return periods' and the Gumbel distribution (Pérez-Bella et al., 2012, 2013). The benefit of this approach is that it is less affected by extreme random weather phenomena and can be applied to sets of event occurrence that have different frequencies of occurrence, e.g. sites and orientations that experience different average quantities of spells per year.

The calculation-based approach of ISO 15927 has the advantage over BS 8104 that WDR may be assessed at any location or time for which appropriate data or predictions are available. However, the indices do not reflect other characteristics of the annual or spell behaviour, including:

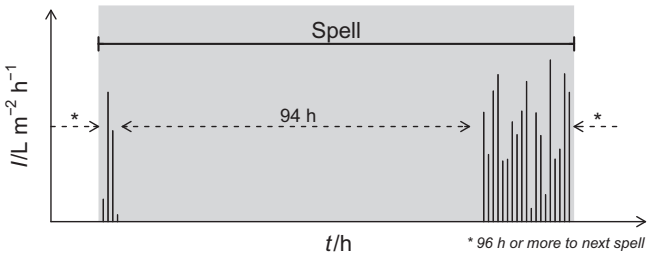

Fig. 1. An example of a driving rain spell, as defined in ISO 15927-3:2009.

- spell duration
- fraction of hours for which there was active wind-driven rain within a spell (the 'active fraction')
- the length of time between sequential spells (inter-spell period)

Some of these additional properties have been discussed for rain spells across the United States (Underwood and Meentemeyer, 1998), but have not been explored for the UK. It should also be noted that output from the semi-empirical model in Eq. (1) does not reflect localised microclimates, such as those common in urban environments. The context of building façade can have a significant impact on the level of exposure, which can be explored with CFD.

2.3. Meteorological data

2.3.1. Baseline period data

As discussed in Section 2.2, long-term hourly data is required to calculate WDR indices. A baseline reference period of 1961–1990 was used, as this closely resembles the period of observations used to formulate BS 8104 (1959–1991) (BSI, 1992) and 1960 is also a frequently used comparison basis for climate projections by the IPCC IPCC (2013). Similarly, 1961–1990 is the basis for the UK Climate Impacts Programme (UKCIP) and the 2009 UK Climate Projections (UKCP09) Weather Generator tool (see Section 2.3.2).

2.3.2. Creation of future probabilistic design weather years

To assess future WDR characteristics, the most recent 2009 UK Climate Projections (UKCP09) have been used to create probabilistic meteorological conditions (DEFRA, 2009) for 2070–2099 under an A1 high emissions scenario. This scenario was selected from the IPCC Special Report on Emissions Scenarios (Nakićenović and Swart, 2000): it characterises a scenario of high fossil fuel use with rapid economic growth and introduction of new and more efficient technologies [Murphy et al., 2009, pp. 134–135].

UKCP09 includes a Weather Generator that is a stochastic rainfall model (Wilks and Wilby, 1999) to produce artificial time series under various emission scenarios – other weather variables are then generated according to the precipitation and inter-variable relationships on the previous day. These relationships contribute to maintaining the consistency between and within each variable (Jones et al., 2009). The Weather Generator creates hundreds or thousands of future 30-year statistically equivalent time series representative of predicted behaviour. The time series represent future characteristics but would not be expected to reflect actual measurements over their respective time horizons. Using 100 or more Weather Generator outputs

[4] Alternative units of the analogous $\mathrm{mm\,h^{-1}}$ are sometimes used. This has not been employed to avoid confusion between the vertical rainfall (precipitation) and the calculated WDR exposure.

allows a range of plausible scenarios to be explored that represent the probability distribution.

The Weather Generator provides generated time series for a baseline period (1961–1990) and the future scenario (2070–2099) for 5 km × 5 km grid cells over the UK. The daily time series contain the following variables, among others:

- precipitation, mm
- maximum temperature, ° C
- minimum temperature, ° C
- sunshine fraction
- vapour pressure, Pa
- potential evapotranspiration (PET), mm day^{-1}

Precipitation, maximum and minimum temperatures, vapour pressure, and radiation parameters are produced at the hourly resolution using simple disaggregation rules from the estimated daily parameters [Jones et al., 2009, p. 31].

Using ISO 15927, hourly time series of wind direction, wind speed, and precipitation are required to evaluate WDR indices. The output from the UKCP09 Weather Generator has been adapted to produce the necessary hourly time series required as input to building simulation software (Du et al., 2012; Mylona, 2012; Watkins et al., 2011). The limitations of the Weather Generator approach is that not all variables required for simulation or calculation purposes are created at the hourly resolution.

Eames et al. have developed a process using probabilistic models to produce the necessary variables for WDR indices at an hourly resolution from the Weather Generator output (Eames et al., 2011a,b). The generation process requires a reference hourly time series with the relevant variables to use as a 'training' data set for the algorithms. In this paper, measured data from the 'Met Office Integrated Data Archive System' (MIDAS) Land and Marine Surface Stations Data (1853–current) (NCAS British Atmospheric Data Centre, 2012) for 1961–1990 was used. This was selected so that it covered the same years as the baseline period. The process can be summarised as:

1. Calculate average daily wind speed from PET (Ekström et al., 2007)
2. Generate 24 h of hourly wind speeds: extract 24 h measurements from the closest average daily wind speed occurring during the same season (DJF, MAM, JJA, SON) in the reference data set
3. Generate 24 h of hourly wind direction: every 6 h, generate a random probabilistic wind direction from the corresponding season and daily wind speed, linearly interpolate between generated values
4. Linearly interpolate between any missing data in the time series

Eames et al. showed this process to reproduce measured data very well for a range of sites across the UK (Eames et al., 2011a,b). This assumes that, in future, the relationships between rainfall volume and other weather variables remains consistent, i.e. greater amounts or frequencies of precipitation will be reflected in proportional increases in wind speeds. Wind directions in the UK are dominated by the south-westerly jet streams: although they have shown significant variability in the twentieth century, there is little evidence to suggest a changing trend over the past few decades (Jenkins, 2007).

This generation process has been validated against the CIBSE Test Reference Years for Plymouth (C. I. for Buildings Services Engineers, 2017), 1983–2004 (Eames et al., 2011a). To assess its applicability to the selected sites, the process was also applied to the 'baseline' scenarios (1961–1990) outputted by the Weather Generator, using the reference (training) data set from the 1961–1990 MIDAS observations (NCAS British Atmospheric Data Centre, 2012) from a nearby site.

2.4. Sites

The UK experiences a temperate oceanic climate (Peel et al., 2007) with a strong influence from the south-westerly polar front jet stream. This causes frequent fluctuations and unsettled weather is typical. Its location between the Atlantic Ocean, continental Europe and the Scandinavian Peninsula causes significant precipitation differences between east and west, especially in coastal regions. Owing to the differences in latitude and the impact of occasional continental tropical air masses from the south, there can be significant thermal differences between northern and southern regions.

Eight sites were selected for this study to represent the geographical variation of built heritage sites in the UK (Fig. 2). Site selection was constrained by the need to have sites with 30 year hourly wind and precipitation data in the MIDAS database (NCAS British Atmospheric Data Centre, 2012). Due to this many of these eight have previously been used as central nodes in maps of driving rain (e.g. BSI, 1992; Prior, 1985) . The selected sites are representative of airfield conditions, i.e. unimpeded by urban canyons and reduced wind and precipitation. It should be noted that there were few locations with data that met the selection criteria in Northern

Fig. 2. Study sites, representing the variability of exposures to precipitation and wind across the UK.

Ireland. It is not suggested that the characteristics of the entire region are characterised by the properties observed for Aldergrove. This is important in the context of the strong winds typically experienced on the west coast of Ireland.

3. Results

3.1. Model validation

Eames et al. (2011a,b) have validated that probabilistic generation processes can be used to produce realistic hourly data series. To assess the applicability of this approach and estimate the error for the selected UK sites, the frequency (occurrence) of different meteorological conditions in the generated baseline data (1961–1990) were compared to the reference data for each site during the same time period.

To assess how similar the generated baseline time series are to the recorded meteorological conditions, the frequency (occurrence) of relevant parameters divided into bins or discrete values is presented in Fig. 3. The parameters with their respective bin sizes and/or discrete value ranges are presented in Table 1. In Fig. 3, the black line 45° denotes a 1:1 ratio, while the red bold line is a logarithmic-transformed least-means correlation weighted according to frequency. How closely these lines lie to one another represents how well the generated data reproduces the characteristics of the measured reference data.

Some variation between the two data sets is to be expected, as the UKCP09 projections are provided at a resolution of 25 km × 25 km regions. Even though the Weather Generator allows for the selection of 5 km × 5 km, the climate predictions at this scale merely present the calculations undertaken at the larger scale. What is important is that the generated baseline data series have similar characteristics to the recorded meteorological data, even if they are not identical.

The most important parameters for calculating driving rain exposure with Eq. (1) are the hourly mean wind speed, hourly precipitation, and predominant hourly wind direction. There is a very good relationship between the generated and down-sampled time series of hourly mean wind speeds and hourly precipitation. This is to be expected for the latter, as these values are a direct output of the Weather Generator. With regards to hourly wind speed, the strong correlation ($R^2_{weighted} = 0.91$) is the result of the probabilistic processes employed by Eames et al., and agrees with their assessments of reproducing wind speeds.

The generated daily precipitation is very similar to the measured daily precipitation. This is similar to the hourly precipitation, as the daily values are also a direct output of the Weather Generator and therefore derived directly from the UK Climate Projections from 2009. The discrepancy between modelled and measured data for both hourly and daily wind speeds is partially explained by the limitations of calculating them using PET, since this value is truncated at 0 (i.e. it cannot be negative) and is only generated to two decimal places (Eames et al., 2011a).

Table 1
The parameters employed to calculate the frequency of different meteorological conditions used in the comparison of the baseline generated time series and the recorded meteorological data.

Parameter	Time resolution	Type	Divisions, Interval
Wind direction	Hourly	Discrete	0° to 350°, 10°
Wind speed	Daily	Bins	0 to 30 m s^{-1}, 1 m s^{-1}
Wind speed	Hourly	Bins	0 to 30 m s^{-1}, 1 m s^{-1}
Precipitation	Daily	Bins	0 to 50 mm h^{-1}, 1 mm h^{-1}
Precipitation	Hourly	Bins	0 to 30 mm h^{-1}, 1 mm h^{-1}

The distributions of wind speeds and precipitation are logarithmic, with low values much more common than high values. Extremes of hourly precipitation are well-reproduced in the generated baseline data sets. This is represented by $R^2_{weighted} = 0.99$, and negligible deviation from the 45° line (representing a 1:1 equivalency). In contrast, the probabilistic approach under-represents extreme hourly wind speeds. This is represented by a lower $R^2_{weighted} = 0.91$, and many parameters bins/discrete values deviating significantly from the diagonal 1:1 equivalency in Fig. 3. It is important to note:

- these extreme high wind speed values occur very rarely, i.e. for less than 100 h in 30 years
- in Eq. (1), an increase of 1 m s^{-1} in hourly wind speed for wind speeds greater than 20 will, at most, modify the WDR exposure by 5%
- The extremes of hourly wind speeds are more pronounced for specific sites: for example, Plymouth (in dark gray points in Fig. 3) consistently deviates further from the 1:1 equivalency, than other sites, i.e. it is the site at which extreme hourly wind speeds are most significantly under-represented

The hourly wind direction warrants discussion, as the wind direction distribution is more regular than the other parameters. The wind directions generated by the Eames algorithm have a unique pattern that can be described as a saw-tooth: alternating higher and lower values for neighbouring wind directions. This is visible in Fig. 4 and in the literature [Eames et al., 2011b, p. 131]. These differences are most likely "due to the simplistic method used, where 1 h is not dependent on the next and because the interpolation does not follow the same probabilistic distribution' [as the other variables]"[Eames et al., 2011b, p. 130]. Despite the saw-tooth pattern, the overall characteristics of site-specific wind directions are reproduced by the

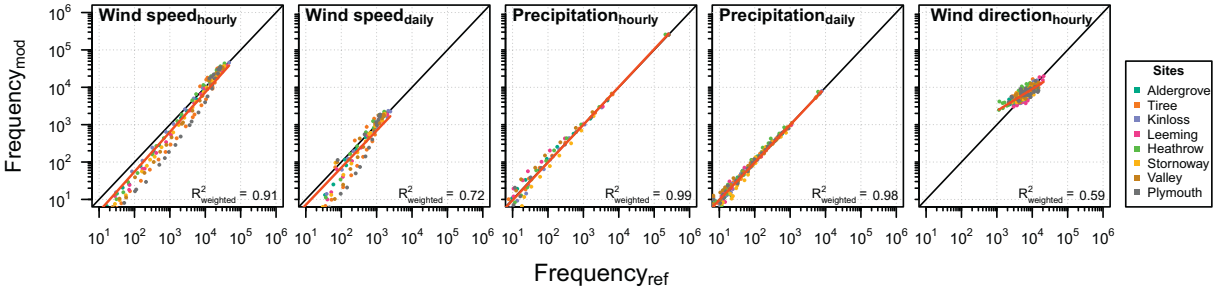

Fig. 3. Comparison of the generated baseline time series (1960–1990) to the recorded meteorological data at sites within their respective prediction regions for eight UK sites. The bin frequency of the wind speed and precipitation is compared (daily and hourly), as well as the hourly wind direction.

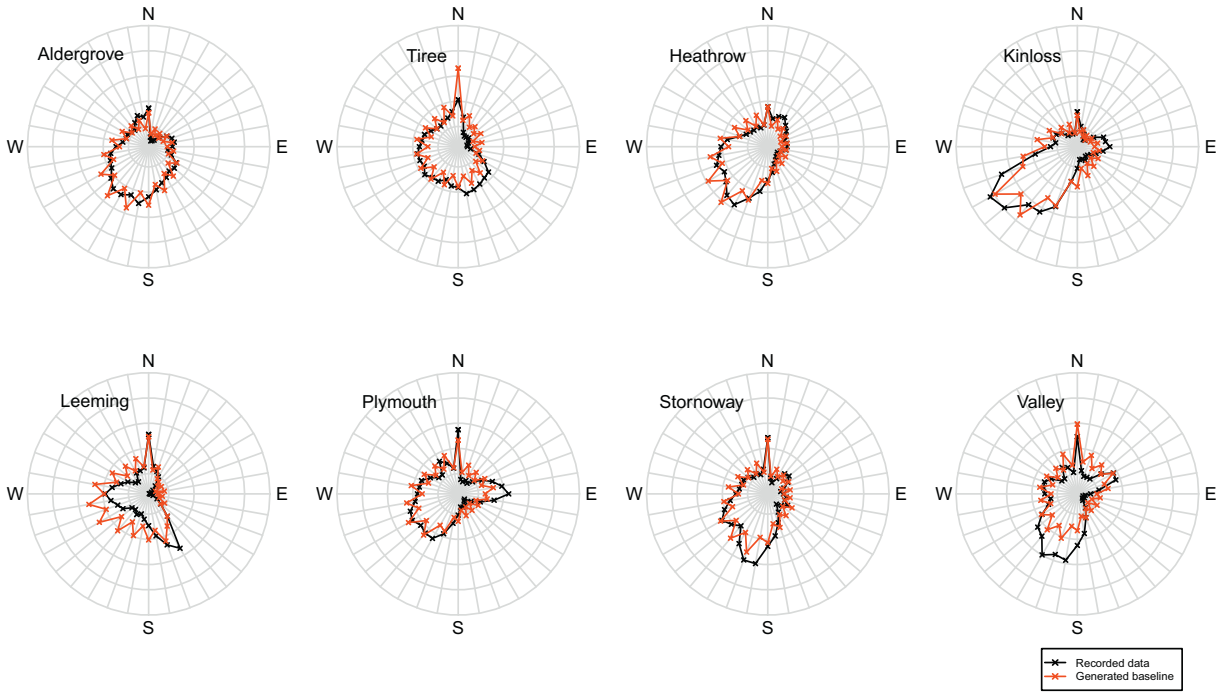

Fig. 4. Comparison of the mean hourly wind speed distribution for the generated baseline time series (1961–1990) to the recorded meteorological data. 0° represents a wind from the north.

probabilistic process. It is useful to note that a 10° difference in wind direction will, on average, change the cosine component (and therefore WDR exposure) of Eq. (1) by 11%.

3.2. Annual characteristics

The sites experienced varying annual WDR exposure during 1961–1990 (Table 2). In general, western coastal sites (Tiree, Stornoway, Valley, Plymouth) have on average received more than 380 L m^{-2} of annual WDR exposure. In contrast, inland and eastern sites in Britain (Kinloss, Leeming, and Heathrow) received less than 240 L m^{-2} of WDR annually. Aldergrove received an annual average WDR exposure of 330 L m^{-2}, which is significantly more than the other inland sites. This likely represents the overall higher exposure in Ireland due to weather systems arriving from the Atlantic Ocean in the west.

The sites with higher baseline WDR volumes are also those that are predicted to change most. This is most prominent in the WDR exposure of western sites of Wales and Scotland: Valley and Tiree. Sites that have had mid-level exposure of roughly 370 L m^{-2} (i.e. Stornoway and Plymouth) are predicted to increase to the low 400s. In contrast, the more inland and eastern sites (Kinloss, Heathrow and Leeming) are not predicted to change very much.

The significant predicted changes in the annual WDR volumes calculated from the data in Table 2 and shown in Table 3 are between 7.2% and 25% for specific sites, but this does not reflect seasonal diversity.

It is generally accepted that, with future climate change, the meteorological conditions within different seasons will change, especially in winter (Hansen and Sato, 2016; Watts et al., 2015). This will also manifest as changes in the characteristics of wind-driven rain. To assess this, the calculated annual indices I_A were separated in Tables 2 and 3 into seasons based on calendar months: winter (DJF), spring (MAM), summer (JJA), autumn (SON). This analysis demonstrates that the predicted change in WDR exposure during different seasons is not proportional to the annual average change (Fig. 5). There are strong polarising contrasts apparent for the winter and the summer, while the predicted changes in spring and autumn are closely related to the annual predicted changes.

The severity of predicted seasonal change is not the same across sites. For example, western coastal sites including Stornoway, Tiree, and Valley are predicted to experience as much as a 40% increase

Table 2
Annual indices (I_A, total exposure to wind-driven rain) during the baseline (1961–1990) and under the prediction scenario (2070–2099) at the eight sites for all wall orientations.

Site	$I_{A,\text{baseline}}$ (1961–1990)					$I_{A,\text{scenario}}$ (2070–2099)				
	Annual	Winter	Spring	Summer	Autumn	Annual	Winter	Spring	Summer	Autumn
	L m^{-2}	L m^{-2}	L m^{-2}	L m^{-2}	L m^{-2}	L m^{-2}	L m^{-2}	L m^{-2}	L m^{-2}	L m^{-2}
Aldergrove	330 ± 8.1	90 ± 3.1	70 ± 1.09	70 ± 1.5	90 ± 3.0	340 ± 9.0	110 ± 3.8	50 ± 1.4	50 ± 1.4	100 ± 3.4
Tiree	540 ± 7.1	180 ± 2.8	100 ± 0.64	80 ± 1.4	180 ± 3.0	680 ± 10	250 ± 4.6	80 ± 1.5	80 ± 1.5	220 ± 4.3
Kinloss	240 ± 6.5	60 ± 2.1	50 ± 1.1	60 ± 1.2	70 ± 2.4	270 ± 8.0	80 ± 2.8	50 ± 1.3	50 ± 1.3	90 ± 3.1
Leeming	210 ± 4.6	60 ± 1.6	50 ± 0.78	40 ± 0.93	60 ± 1.7	210 ± 4.8	60 ± 1.9	40 ± 0.93	40 ± 0.93	60 ± 1.7
Heathrow	200 ± 3.9	60 ± 1.2	50 ± 0.52	40 ± 0.91	60 ± 1.4	200 ± 4.2	70 ± 1.5	30 ± 0.96	30 ± 1.0	60 ± 1.6
Stornoway	390 ± 8.0	140 ± 2.8	80 ± 1.2	60 ± 1.7	110 ± 2.5	400 ± 8.7	170 ± 3.9	40 ± 1.5	40 ± 1.5	100 ± 2.7
Valley	520 ± 10	170 ± 4.7	110 ± 1.1	80 ± 0.84	160 ± 4.2	620 ± 13	220 ± 6.4	70 ± 0.93	70 ± 0.96	200 ± 5.5
Plymouth	380 ± 6.1	120 ± 2.1	70 ± 0.70	60 ± 1.3	120 ± 2.3	410 ± 6.9	150 ± 2.8	50 ± 1.3	50 ± 1.3	130 ± 2.8

Table 3
Predicted change in the annual spell index I_A (total wind-driven rain exposure) from 1961–1990 to 2070–2099 for all wall orientations. Italics indicate that the predicted change are statistically insignificant within a 95% CI.

Site	Annual %	Winter %	Spring %	Summer %	Autumn %
Aldergrove	5.8 ± 5.3	21 ± 7.4	*2.7 ± 3.1*	−18 ± 4.3	10 ± 6.8
Tiree	25. ± 3.2	40 ± 4.1	22 ± 2.1	−3.7 ± 3.5	24 ± 4.1
Kinloss	13 ± 6.1	24 ± 8.0	9.5 ± 4.4	−7.3 ± 4.6	23 ± 7.9
Leeming	*0 ± 4.6*	16 ± 6.2	*1.3 ± 3.4*	−18 ± 4.2	*−2.3 ± 5.9*
Heathrow	*3.6 ± 4.1*	23 ± 4.9	*0.38 ± 2.4*	−18 ± 4.8	*1.8 ± 5.4*
Stornoway	*3.3 ± 4.3*	25 ± 4.8	*1.2 ± 3.1*	−29 ± 5.5	−6.0 ± 4.8
Valley	18 ± 4.6	27 ± 6.4	14 ± 2.4	−10 ± 2.3	23 ± 5.9
Plymouth	7.2 ± 3.4	22 ± 4.0	5.3 ± 2.1	−22 ± 4.1	8.6 ± 4.2

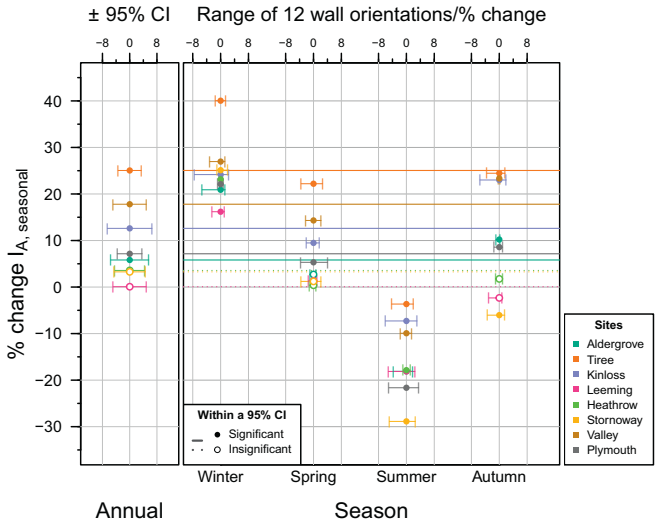

Fig. 5. The predicted changes in average exposures of wind-driven rain, presented for annual behaviour and for individual seasons.

in WDR volume during the winter months. It is also predicted that Stornoway could experience almost 30% less WDR in the summer months, and slightly lower than annual exposures during the autumn.

3.3. Spell volumes

The volume of water hitting surfaces during wind-driven rain spells is predominantly increasing. The intensity (or volume hereafter) of WDR spells during the winter, spring, and autumn is predicted to increase, while extreme events – such as the worst spell likely to occur in a three year period I_S– are predicted to increase by greater amounts. For some sites, the summer months will have lower WDR exposure with regards to both general and extreme behaviour. At other sites, this change is insignificant. As established in BS 8104 and its preceding publications, façades facing the south-west will be more exposed to WDR, as they are more frequently hit by prevailing wind directions in the UK.

The worst spell likely to occur once every three years I_S is predicted to increase by 22% and 59% at specific sites (Table 4). Similarly, the mean exposure of spell-specific indices ($I_{S,mean}'$) is also predicted to increase, but by between 4.8% and 27%. This means that while larger differences are predicted in extreme events, the average WDR exposure is also predicted to increase.

Section 3.2 established the importance of assessing WDR exposures seasonally. This is also important for an assessment of the predicted characteristics of WDR spells. Fig. 6 shows the volumes of the mean and the worst spell likely to occur at each site once every three years during different periods. When spells occurred over the duration of two seasons, they were categorised to the season in which most of the spell occurred. As established for the annual behaviour, annual predicted changes in spell exposure are not capturing the differences between seasons. Notably, summer extreme events are predicted to become less intense, although this is insignificant for some sites and/or wall orientations.

During the baseline period 1961–1990, the worst spell likely to occur once every three years is likely to occur during the winter or autumn months. For this reason, there is little difference between these periods of time in Fig. 6. In contrast, the extreme spell volumes occurring in spring and summer are significantly less severe.

As Fig. 6 demonstrates, there are significant differences in spell volumes for different wall orientations during the baseline period. However, the predicted changes in volume for each wall orientation are similar to those presented in Table 4. This means that all façades of a building are predicted to see a similar percent change in their exposure, which will be varying severity depending on the established directional characteristics of WDR exposure.

Western sites have the highest baseline and predicted 'once every three year' spells, but these sites also have much higher mean I_S WDR exposures than their eastern and inland counterparts. The extreme event exposures (such as I_S) and the mean WDR exposure are not directly proportional. While there is a general relationship between the two, the volume of the mean WDR exposure varies relative to the 'once every three year' exposure. The predicted changes as percentages in the mean I_S' and the 'once every three year' spell volumes are much more similar, suggesting a common driving force that is likely annual precipitation.

3.4. Spell durations and inter-spell characteristics

Shorter wind-driven rain spells are predicted to become more common, with more time elapsing between them (Fig. 7). Spells less than 10 h in duration were the most common type between 1961–1990, and they are predicted to occur much more frequently in the 2070–2099 scenario. For most locations, there is insignificant or

Table 4
Predicted percent change in exposures to wind-driven rain from 1961–1990 to 2070–2099, for all wall orientations.

	Mean spell-specific index $I_{S,mean}'$					Once every three years spell I_S				
	Annual	Winter	Spring	Summer	Autumn	Annual	Winter	Spring	Summer	Autumn
Aldergrove	4.8 ± 1.9	23 ± 4.2	*−3.2 ± 3.3*	−21 ± 4.5	15 ± 4.4	23 ± 5.4	24 ± 7.9	*5.5 ± 6.5*	*−7.7 ± 9.5*	18 ± 7.8
Tiree	27 ± 4.1	44 ± 8.3	16 ± 5.1	*−3.4 ± 5.0*	46 ± 9.1	54 ± 8.5	55 ± 11.1	32 ± 8.9	*2.0 ± 8.9*	45 ± 10
Kinloss	13 ± 2.9	25 ± 4.6	10 ± 4.4	−10 ± 4.9	27 ± 6.8	29 ± 7.4	36 ± 11	21 ± 8.3	*6.2 ± 8.8*	25 ± 9.4
Leeming	4.8 ± 2.2	20 ± 4.9	*3.4 ± 4.0*	−12 ± 4.7	*3.8 ± 4.4*	*11 ± 27*	*17 ± 29*	9.0 ± 6.9	*−7.1 ± 9.8*	*4.4 ± 8.2*
Heathrow	13 ± 2.4	27 ± 4.7	*3.1 ± 3.8*	2.9 ± 6.5	11 ± 4.3	22 ± 5.2	27 ± 7.5	15 ± 8.0	11 ± 10	16 ± 8.3
Stornoway	8.0 ± 3.2	15 ± 5.1	*1.5 ± 4.2*	−18 ± 4.8	23 ± 6.7	30 ± 7.7	30 ± 9.4	*8.4 ± 8.8*	−13 ± 7.7	30 ± 8.5
Valley	13 ± 2.4	23 ± 4.8	7.6 ± 3.3	−10 ± 5.1	12 ± 5.0	24 ± 6.3	30 ± 9.1	21 ± 8.4	*−2.4 ± 9.9*	13 ± 8.4
Plymouth	14 ± 3.4	37 ± 7.3	*3.8 ± 4.0*	−12 ± 5.9	*2.0 ± 4.2*	25 ± 7.4	28 ± 9.7	22 ± 9.4	*−1.1 ± 13*	7.6 ± 7.9

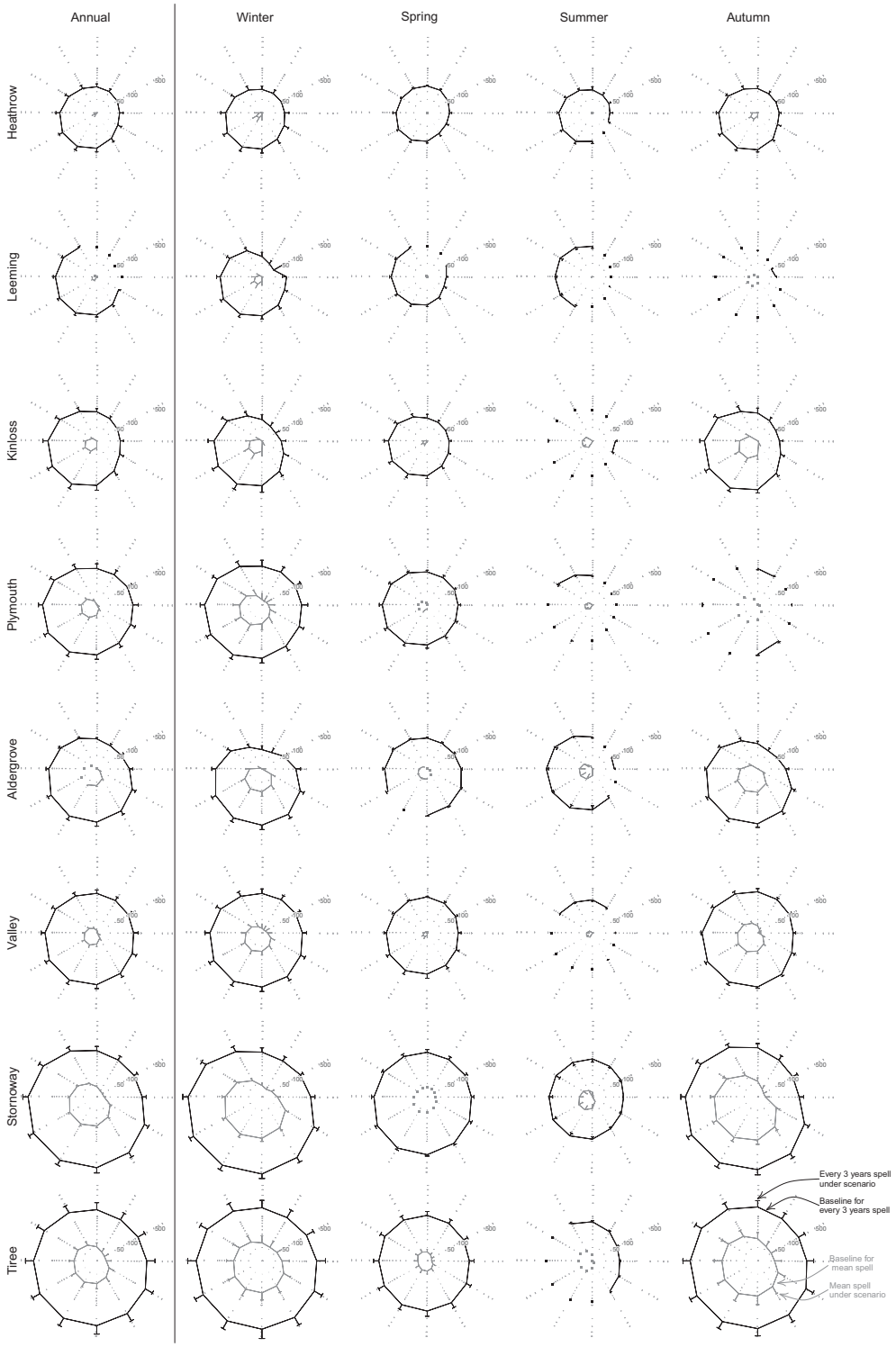

Fig. 6. The volumes of the mean and the worst spell likely to occur once every three years at each site during different periods, represented by the gray and black circles, respectively. The whiskers indicate the predicted conditions in 2070–2099; unconnected points indicate change that was not significant within a 95% CI. The radial directions indicate wall orientations, where North = 0°.

slightly negative change in the occurrence of spells of medium length (lasting more than 10 h but less than 100 h). Longer spells (durations greater than 100 h) are predicted to occur much less frequently. Stornoway is unique in that mid-length spells (lasting more than 10 h but less than 100 h) are predicted to become much more common.

By definition, the minimum spell duration is the resolution of the meteorological measurements inputted into Eq. (1), i.e. 1 h. The theoretical maximum duration for a rain spell (by the definition in ISO 15927) is the duration of the input meteorological data. In practice, rain spells very rarely extended beyond 1000 h. The few outlying spells that exceed 1000 h have been removed from the statistics presented herein – in general, they are found in regions with higher annual precipitation where gaps of 96 h or more without any WDR exposure are less common.

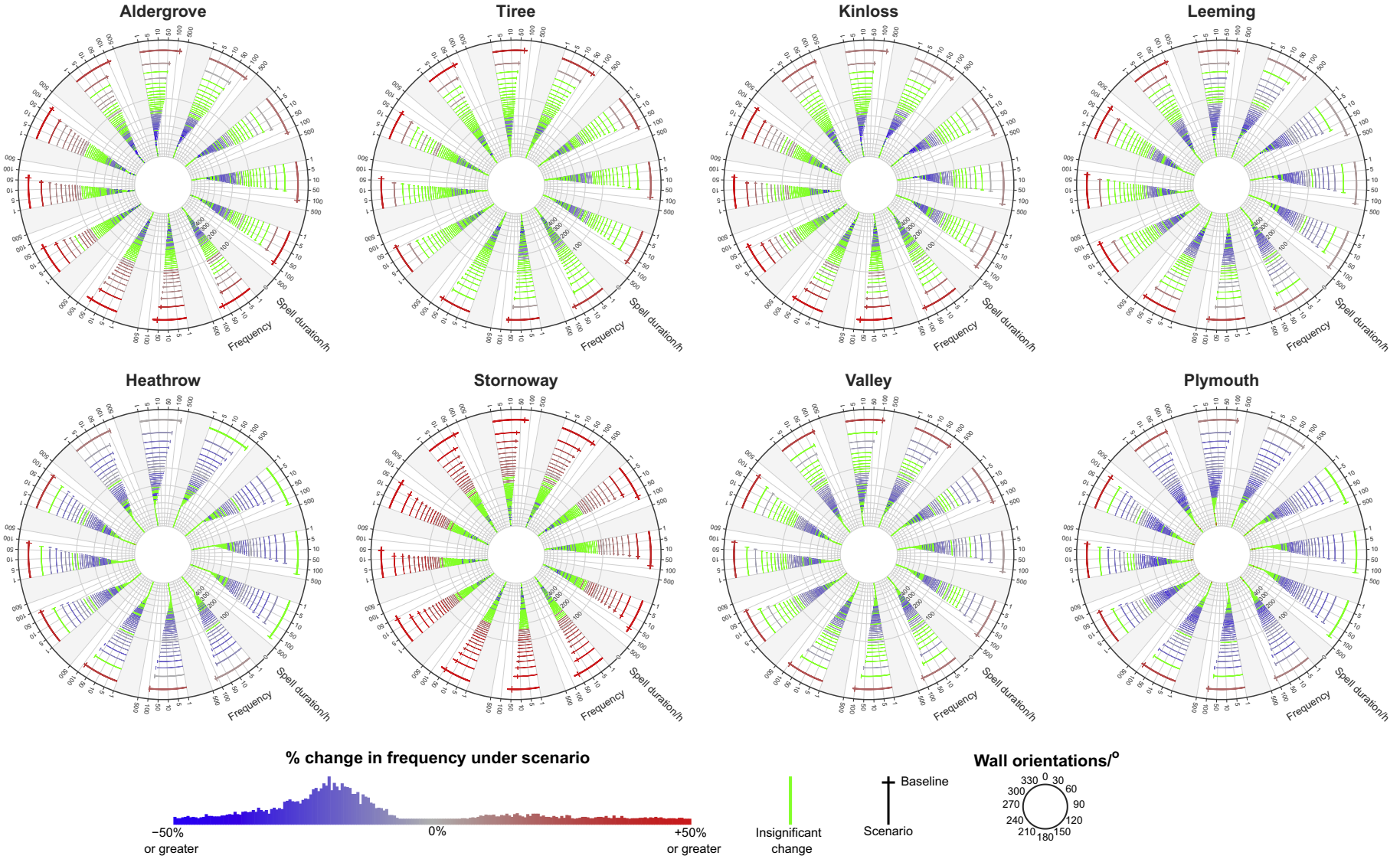

Fig. 7. The frequency of wind-driven rain spells of different lengths at eight UK sites. The 12 'sub-axes' within each polar plotting area represent wall orientations (North = 0°). The 10 h bins are plotted as radial lines representing their mid-point, e.g. 5, 15, …, 995 h. The perpendicular axis represents the spell duration, and the radial axis represents their frequency of occurrence. The main line of the radial axis is the frequency under the predicted scenario, while the cross-line of the 't' is the baseline. The colour scale shows the predicted percentage change of frequency for the spell duration bins: red for increase, blue for decrease (with gray representing no change). Green is used to show when the change in occurrence was statistically insignificant.

Fig. 7 shows the frequency in occurrence of spells of different lengths, in which each polar plot represents one site. The twelve axes within the polar plot represent wall orientations (see key in Fig. 7). At all sites and wall orientations, the predicted change in occurrence of spells longer than 500 h is predominantly statistically insignificant. This is likely because they occur much less often than shorter spells.

There is little change predicted for the number of spells occurring per year at each site and wall orientation (approximately 2–3 spells per year, equivalent to less than 10%, at most, and insignificant for 3 of the sites). For the UK, a site and wall orientation, on average, experiences 23 rain spells (as defined by ISO 15927) for 1961–1990 and not predicted to change over the twenty-first century. Natural variation around this average is caused by two factors: annual precipitation and prevailing wind directions. For regions that experience higher than average annual precipitation, there are less likely to be periods of 96 h or longer without driving rain, so subsequent depressions would be bridged into a single spell. Also, walls oriented to be hit by prevailing UK wind patterns will less frequently meet the aforementioned condition for dividing exposure into spells.

If rain spells are predicted to become shorter but occur with the same annual frequency, it follows that there will be longer periods of time between them. Table 5 presents two metrics for quantifying this: the mean period of time elapsing between sequential WDR spells, and the fraction of hours that were within rain spells on average out of the total number of hours occurring in a one-year period.

It can be observed that the inter-spell periods are increasing, on average, by approximately 1 day, representing a 10–15% increase in 2070–2099 upon 1961–1990. A concomitant decrease can be observed in the number of hours within an annual period that are within rain spells, as opposed to inter-spell periods.

3.5. Intra-spell characteristics

At all sites, regardless of spell length, the fraction of hours within spells during which there is WDR exposure occurring, the ‘active fraction’ is predicted to increase — except for long spells at Plymouth, which are predicted to decrease negligibly. The most significant increases in the active fraction are predicted to occur for the mid-length spells (longer than 10 h but less than 100 h long).

Sections 3.3 and 3.4 present predicted increases in the volume of rain spells and decreases in their duration. While these affect the wind-driven rain exposure at the single-spell level, they do not consider how the exposure might be distributed *within* an individual WDR spell.

To assess this, it is interesting to consider the ‘active’ fraction, defined as the number of hours within a rain spell during which there is exposure to wind-driven rain for a given location and wall orientation. Table 6 shows the active fraction at each site for short, medium, and long WDR spells.

The active fractions for short spells are approximately 0.90, while for medium and long spells they are about 0.30 and 0.15, respectively. Longer spells have lower active fractions than their shorter counterparts, as they are more likely to bridge between multiple weather depressions but have periods with no WDR within them.

4. Discussion

Two points of discussion are necessary: a review of some of the factors that impact the semi-empirical calculations of WDR and predictions of wind-driven rain (Section 4.1), and a consideration of the implications of the predictions for cultural heritage and built infrastructure (Section 4.2). An important part of the latter is to highlight aspects of wind-driven rain that are not captured by the current standard metrics – imperative to characterising future risk if they are predicted to significantly change in frequency of occurrence and/or severity.

4.1. Factors impacting calculations and predictions of wind-driven rain

The predictions in this paper are based on a multi-stage method. Each of these stages has implicit assumptions, caveats, and/or limitations.

4.1.1. Availability and applicability of meteorological data

ISO 15927 requires at least 10 years (and ideally 20–30 years) of hourly meteorological data to account for annual variability of wind-driven behaviour. As a reference time frame of 1961–1990 was selected to be the same as the baseline provided by the UKCP09, sites with data fulfilling the criteria were limited. The weather station data used may not be representative of the grid used in UKCP09, and will also not accurately reflect the microclimates created in urban environments.

4.1.2. Limitations of the Weather Generator and the probabilistic generation of future weather timeseries

A report on the UKCP09 Weather Generator specifies that the fitted data “must be validated by the user” [Jones et al., 2009, p. 31]. Section 3.1 demonstrated the time series created from the Weather Generator data did not simulate extremes of high wind speeds, which is also an acknowledged attribute of the Weather Generator Jones et al. (2009). It should also be considered that both the Weather Generator and the Eames probabilistic process are *learning* methods that lack a physical basis; therefore, any use of a training data set (e.g. one from 1961–1990) assumes that certain relationships and characteristics of the climate are also applicable for the future time periods of interest. Finally, the Weather Generator is “based on two models with time scales of one day to one month. The models are made to follow the average seasonality… but variability on time scales longer

Table 5
Period of time elapsing between sequential wind-driven rain spells from 1961–1990 and 2070–2099, with changes. The mean fraction of hours within rain spells represents the fraction of hours that were within rain spells on average out of the total number of hours occurring in a one-year period. All changes are statistically significant within a 95% CI.

	Mean inter-spell period			Mean fraction of hours within rain spells		
	1961–1990 h	2070–2099 h	Change h	1961–1990 –	2070–2099 –	Change %
Aldergrove	180 ± 0.49	200 ± 2.6	26 ± 3.1	0.51 ± 0.002	0.43 ± 0.01	−15 ± 2.1
Tiree	170 ± 0.46	180 ± 1.9	14 ± 2.4	0.60 ± 0.002	0.57 ± 0.01	−5.0 ± 2.3
Kinloss	200 ± 0.66	220 ± 2.5	21 ± 3.2	0.42 ± 0.002	0.36 ± 0.01	−14 ± 2.1
Leeming	210 ± 0.89	240 ± 3.9	30 ± 4.8	0.37 ± 0.003	0.31 ± 0.01	−15 ± 3.6
Heathrow	220 ± 0.67	260 ± 4.4	34 ± 5.1	0.31 ± 0.001	0.27 ± 0.01	−11 ± 3.1
Stornoway	160 ± 0.54	180 ± 1.6	16 ± 2.2	0.65 ± 0.002	0.58 ± 0.01	−11 ± 1.0
Valley	180 ± 0.52	210 ± 2.8	28 ± 3.4	0.44 ± 0.002	0.38 ± 0.01	−12 ± 2.3
Plymouth	200 ± 0.61	240 ± 4.6	34 ± 5.2	0.37 ± 0.002	0.34 ± 0.01	−9.0 ± 3.2

Table 6
Mean fraction of hours within spell with wind-driven rain.

	Short spells (less than 10 h)			Mid-length spells (longer than 10 h but less than 100 h)			Long spells (greater than 100 h)		
	1961–1990 –	2070–2099 –	Change %	Baseline –	2070–2099 –	Change %	1961–1990 –	2070–2099 –	Change %
Aldergrove	0.89 ± 0.0016	0.92 ± 0.0026	3.3 ± 0.48	0.26±0.0013	0.28±0.0041	10 ± 2.1	0.13 ± 0.0003	0.14 ± 0.0013	4.9 ± 1.2
Tiree	0.87 ± 0.0019	0.92 ± 0.0032	5.3 ± 0.58	0.28±0.0012	0.31±0.0037	11 ± 1.8	0.14 ± 0.0003	0.15 ± 0.0011	5.2 ± 2.0
Kinloss	0.92 ± 0.0014	0.93 ± 0.0025	1.5 ± 0.42	0.22±0.0010	0.26±0.0036	20 ± 2.1	0.12 ± 0.0003	0.13 ± 0.0012	12 ± 1.3
Leeming	0.90 ± 0.0013	0.91 ± 0.0029	1.6 ± 0.47	0.24±0.0009	0.26±0.0036	11 ± 1.9	0.12 ± 0.0004	0.12 ± 0.0011	3.5 ± 1.2
Heathrow	0.89 ± 0.0012	0.92 ± 0.0030	3.3 ± 0.47	0.27±0.0009	0.29±0.0034	8.6 ± 1.6	0.13 ± 0.0004	0.13 ± 0.0012	3.4 ± 1.3
Stornoway	0.89 ± 0.0020	0.92 ± 0.0031	2.7 ± 0.56	0.25±0.0014	0.29±0.0036	19 ± 2.0	0.14 ± 0.0003	0.15 ± 0.0009	7.4 ± 0.91
Valley	0.89 ± 0.0013	0.92 ± 0.0025	3.6 ± 0.42	0.29±0.0012	0.32±0.0039	9.0 ± 1.7	0.14 ± 0.0003	0.14 ± 0.0012	3.2 ± 1.1
Plymouth	0.91 ± 0.0012	0.93 ± 0.0030	3.1 ± 0.46	0.32±0.0012	0.33±0.0049	5.0 ± 1.9	0.15 ± 0.0004	0.15 ± 0.0016	−1.7 ± 1.3

than a few weeks is not explicitly represented" [Jones et al., 2009, p. 32]. As rain spells lasting longer than a few weeks rarely occur, the effect of this on the accuracy of the predictions is minimal.

4.1.3. Applicability of ISO 15927-3:2009

The methods in this standard are not applicable for [ISO, 2009, p. 1]: a) mountainous areas with sheer cliffs or deep gorges, b) areas in which more than 25% of the annual rainfall comes from severe convective storms, and c) areas and periods when a significant proportion of precipitation is made up of snow or hail. Additional guidance is provided for data quality: a) indices calculated from inland stations are not representative of buildings in coastal locations (i.e. situated less than 8 km from the sea), b) in mountainous terrain calculated indices apply only to the immediate neighbourhood of the station, c) in predominantly flat regions (i.e. with variations in altitude less than 100 m), the calculated indices are valid up to 100 km from the measurement station. In hilly regions, the limits to validity are much less. It is not thought that any of the study sites should be discounted for these reasons.

4.1.4. Cosine rule

The cosine rule is used in semi-empirical calculations of wind-driven rain to incorporate the angle between the prevailing wind direction and wall orientation. A comparison of the cosine rule and numerical simulations of WDR exposure on building façades showed that it tends to overestimate WDR exposure at higher angles, and is not well-suited for "light to moderate horizontal rainfall intensities and for the higher wind-speed values" [Blocken and Carmeliet, 2006, p. 1188]. Despite these shortcomings, it remains the current standard for incorporating wall orientation into semi-empirical evaluation of WDR exposure.

4.1.5. Effect of droplet diameter

The wind-driven rain index assumes a rain-drop diameter of 1.2 mm, from which the coefficient in Eq. (1) by the inverse of the terminal velocity $V_T = 4.5\ \mathrm{m\,s^{-1}}$. Depending on the type of precipitation (e.g. drizzle, cloudbursts, etc.…) the WDR coefficient can vary as much as 50–200%, which can result in a halving or doubling the WDR exposure within that hour as calculated herein Straube and Burnett (1998). Future work is needed to explore whether information on the predominant type of hourly rainfall can be extracted from meteorological metadata, such as weather codes used by the Met Office. From this, a more accurate droplet diameter could be inferred, increasing the accuracy of semi-empirical representations of WDR.

4.2. Implications for risks to cultural heritage and built infrastructure

Characterising the properties of wind-driven rain spells in the future is an important component of understanding climate change risk. Moreover, the potential effects on built heritage should be inferred, to inform efficient and effective management of change.

The metrics used in current standards for assessing wind-driven rain exposure in the UK are relevant to two types of impact:

1. Annual index I_A: for assessing the average moisture content of masonry BSI (1984) and when "assessing the likely growth of messes and lichens" [BSI, 1992, p. 4]
2. Spell index I_S: indicates the likelihood of rain penetration through masonry and joints in other walling systems (ISO, 2009)

For both metrics, the risk is characterised by the volume of water calculated to impact a standard surface area. When considering the potential risks of wind-driven rain, it is proposed that there are three important properties of rain spells: a) volume of the exposure, b) the duration of the spell, and c) the active fraction – the fraction of hours within a spell for which there is actively exposure to wind-driven rain.

It is also important to consider run-off in considering the implications of these changes. The semi-empirical methods for calculating WDR are only applicable up to the point where WDR conceptually impacts a surface. They do not suggest that all of this water is absorbed by the surface, as some of it will likely run over the surface. This has ramifications for the performance of building elements besides porous materials and will be discussed later in this section.

It is useful to consider the four categories of activity related to building performance presented in Table 7 and how these might change under future scenarios: building element failure, biological impacts, cycling, and deep-seated wetting. These activities are directly related to the properties of WDR spells. While there are many other mechanisms that can affect porous building materials and the building envelope – such as salt crystallisation and freeze-thaw effects – their relationships with WDR are more complex and cannot be so easily summarised. Table 7 and the discussions that follow demonstrate the necessity to consider additional characteristics of WDR rain spells in order to categorise the range of potential impacts on cultural heritage.

4.2.1. Applicability of current metrics

I_A is a catch-all metric that ambiguously represents many different kinds of impacts of wind-driven rain. The average annual wind-driven rain exposure is reflective of all types of spells, regardless of their duration and/or active fraction. By definition, it is weighted more heavily towards spells.

I_S is a metric for assessing the potential occurrence of water penetration through masonry and joints. It is defined as the "worst spell likely to occur once every three years", represented by a percentile of all spell exposures of the entire data set. By this definition, I_S reflects

Table 7
Likely change in predicted occurrence of mechanisms impacting building performance in 2070–2099 due to changes in wind-driven rain spells and temperature under a high emissions scenario.

Category	Mechanism of impact	Temperature[a]	Relevant properties of WDR spells				Likely change in predicted occurrence
			Volume	Duration	Inter-spell periods	Active fraction	
Building element failure	Ingress through junctions, cracks, etc…); Failure of moisture management systems (e.g. gutter overspill)	Negligible	Proportional	Inversely proportional	Inversely proportional	Proportional	Increase during winter, spring, and autumn months
Near-surface cycling	Repeated ingress and evaporation of water causing cycles of crystallisation and dissolution of soluble salts	Proportional; higher potential evaporation	Proportional	Inversely proportional	Proportional	Proportional for medium and long spells	Increases
Deep-seated wetting	Penetration through masonry to the interior; thermal bridging (Künzel and Kiessl, 1996); hygric and hydric swelling	Negligible	Proportional	Proportional	Inversely proportional	Proportional	Increase during winter, spring, and autumn months

[a] High emissions scenario for 2070–2099, UKCP09.

spells in which high quantities of water impact a surface. In practice, the spell that this percentile reflects is a spell of a very long duration, as there are more hours in which wind exposure can occur. This does not account for the relatively low active fraction that longer spells (greater than 100 h in duration) typically have: between 10–15%. Penetration through masonry units is more likely to occur during shorter – but more intense – spells, when sequential exposures to quantities of wind-driven rain exert pressures onto existing moisture within porous building materials, driving them deeper into the building envelope.

4.2.2. Building element failure

ISO 15927 acknowledges that the metrics defined within it do not encompass all potential impacts of wind-driven rain: for example, it specifies that building element failure, such as "rain penetration around the edges of doors and windows or similar cracks in building façades… depends on shorter periods of heavy rain and strong winds" [ISO, 2009, p. v]. The failure of building elements could also be expanded to include the effects that follow on from overburdened drainage and moisture management systems. This could be due to insufficient maintenance and/or because the volume of WDR exposure in a given time frame exceed their capacity. When the building elements do not function properly, it can increase the amount of water that runs over a façade, which is often localised to particular areas of a construction.

Such instances are predicted to become more frequent, given that shorter rain spells (less than 10 h) are predicted to become more frequent and more intense. As these spells usually have WDR occurring in most of the hours within their duration (i.e. a high active fraction), there is little time for drainage systems and other building elements to shed water. Metrics are needed that can identify the risks of wind-driven rain to building element failure.

4.2.3. Near-surface cycling

Within standards for wind-driven rain assessment, the period between spells is defined as a minimum of 96 h as it is possible that periods up to this length with no driving rain are necessary before evaporative losses will exceed the ingress from rain exposure (Prior, 1985). While this represents the extreme scenario (and is, to a degree, arbitrary), surface evaporation is likely occurring within spells during the hours in which there is not wind-driven rain exposure – in addition to the inter-spell periods. Such movements of vapour and liquid water can be considered as moisture cycling, both at a micro-scale (within mm from the surface interface) and at the bulk scale.

The distribution of active hours within spells has not been assessed. Although the total fraction of active hours within spells is predicted to increase, further work is needed to understand how clustering or spreading of active hours within rain spells could lead to higher rates of micro-cycling of moisture at the surface and near the surface. Another important component of this analysis would be to consider sub-hourly distributions of rainfall, which could further support moisture micro-cycling.

It is predicted that longer periods of time will elapse between spells, increasing, on average, by roughly one day across all eight UK sites studied here. This could allow for more significant cycling to occur between spells: for example, simple modelling of stone masonry walls shows that 24 h of evaporative drying can mean 0–3 mm [$L\,m^{-2}\,day^{-1}$] of potential evaporation (Hall et al., 2011).

4.2.4. Deep-seated wetting

Deep-seated wetting can be considered as a migration of moisture to and from depth within a masonry construction (Smith et al., 2011). Smith et al. have highlighted the polarising behaviour between the wetness and dryness of winter and summer months that support an increased potential for seasonal-dependent deep-seated wetting.

This would be propagated by an increase of active hours within mid-length and long spells, which could provide more opportunities for moisture gradients to be forced deeper into masonry. In contrast, longer spells are predicted to become less frequent, with longer periods of time between them. It is difficult to postulate which of these effects might dominate, but future work could attempt to model the potential evaporation and moisture ingress under various scenarios.

When it comes to assessing the potential for deep-seated wetting using the current definition of the airfield annual index in ISO 15927 and BS 8104, these changes are being smoothed by an annual average, which is predicted to be 'net positive' for most sites, as the increases during winter months outweighs the decreases predicted for the summer months. Future WDR exposure should be calculated as seasonal indices, as these will more accurately capture the overall exposures to wind-driven rain. Annual and seasonal exposures for the baseline and scenario time periods are presented in Table 2, along with what these represent as percent changes (Table 3). The polarisation of winter and summer volumes strongly suggests that deep-seated wetting will likely become more serious and frequent for western sites in Scotland and Wales.

5. Conclusion

This study has evaluated the projected characteristics of WDR spells and exposure for eight UK sites towards the end of the twenty-first century under a high-emissions scenario. It was shown that the future UK climate is predicted to experience shorter wind-driven rain spells with higher volumes of exposure in more concentrated time periods, especially during winter and autumn months. These increases will be more severe for western and coastal locations that already experienced higher WDR exposure during the twentieth century. The projected impact on building exposure are higher frequency and severity of building element failure, near-surface cycling, and deep-seated wetting.

Combining probabilistic hourly time series generation with semi-empirical formulae of WDR exposure was a robust approach of assessing future exposure. The results demonstrated that there will not only be changes in the quantity of exposure to WDR, but also in the temporal characteristics such as the length of WDR spells and the distribution of exposure within them.

Acknowledgements

Funding: This work was supported by the UK Engineering and Physical Sciences Research Council (EPSRC) grant for the Centre for Doctoral Training Science and Engineering in Art, Heritage and Archaeology (EP/L016036/1). We acknowledge the support of the Natural Sciences and Engineering Council of Canada (NSERC), funding reference number PGSD3-471105-2015. We would like to thank Jennifer Richards and Katherine Jang for their input on an early draft.

References

ASHRAE, 2009. Standard 160-2009 - Criteria for Moisture-control Design Analysis in Buildings. ASHRAE.

Blocken, B., Carmeliet, J., 2004. A review of wind-driven rain research in building science. J. Wind Eng. Ind. Aerodyn. 92 (13), 1079–1130. https://doi.org/10.1016/j.jweia.2004.06.003.

Blocken, B., Carmeliet, J., 2006. On the validity of the cosine projection in wind-driven rain calculations on buildings. Build. Environ. 41 (9), 1182–1189.

Blocken, B., Carmeliet, J., 2007. Validation of cfd simulations of wind-driven rain on a low-rise building facade. Build. Environ. 42 (7), 2530–2548.

Briggen, P., Blocken, B., Schellen, H., 2009. Wind-driven rain on the facade of a monumental tower: numerical simulation, full-scale validation and sensitivity analysis. Build. Environ. 44 (8), 1675–1690. https://doi.org/10.1016/j.buildenv.2008.11.003.

Brimblecombe, P., 2014. Refining climate change threats to heritage. J. Inst. Conserv. 37 (2), 85–93. https://doi.org/10.1080/19455224.2014.916226.

BSI, 1970. BS 4315-2:1970 - Methods of Test for Resistance to Air and Water Penetration. Permeable Walling Constructions (Water Penetration), Standard. British Standards Institution.

BSI, 1984. DD93:1984 - Method for Assessing Eposure to Wind-Driven Rain. British Standards Institute.

BSI, 1992. BS 8104:1992 - Code of Practice for Assessing Exposure of Walls to Wind-Driven Rain, Standard. British Standards Institution.

BSI, 2001. BS EN 12865:2001 - Hygrothermal Performance of Building Components and Building Elements. Determination of the Resistance of External Wall Systems to Driving Rain Under Pulsating Air Pressure, Standard. British Standards Institution.

Cassar, M., 2005. Climate Change and the Historic Environment. Tech. rep., Centre for Sustainable Heritage, University College London, London.

Charola, A.E., Ware, R., 2002. Acid deposition and the deterioration of stone: a brief review of a broad topic. Geol. Soc. Lond., Spec. Publ. 205 (1), 393–406.

Choi, E., 1993. Simulation of wind-driven-rain around a building. Computational Wind Engineering 1. Elsevier., pp. 721–729.

Crispim, C., Gaylarde, C., 2005. Cyanobacteria and biodeterioration of cultural heritage: a review. Microb. Ecol. 49 (1), 1–9. https://doi.org/10.1007/s00248-003-1052-5.

DEFRA, 2009. UK climate projections 2009 [cited 6 September 2017]. http://ukclimateprojections.defra.gov.uk/.

Doehne, E., 2002. Salt weathering: A selective review. In: Siegesmund, S., Vollbrecht, S., Weiss, T. (Eds.), Natural stone, weathering phenomena, conservation strategies and case studies. vol. Special Publication 205. Geological Society of London, pp. 51–64.

Du, H., Underwood, C., Edge, J., 2012. Generating design reference years from the UKCP09 projections and their application to future air-conditioning loads. Build. Serv. Eng. Res. Technol. 33 (1), 63–79.

Eames, M., Kershaw, T., Coley, D., 2011a. The creation of wind speed and direction data for the use in probabilistic future weather files. Build. Serv. Eng. Res. Technol. 32 (2), 143–158.

Eames, M., Kershaw, T., Coley, D., 2011b. On the creation of future probabilistic design weather years from UKCP09. Build. Serv. Eng. Res. Technol. 32 (2), 127–142.

Ekström, M., Jones, P., Fowler, H., Lenderink, G., Buishand, T., Conway, D., 2007. Regional climate model data used within the swurve project? 1: projected changes in seasonal patterns and estimation of pet. Hydrol. Earth Syst. Sci. Discuss. 11 (3), 1069–1083.

Erkal, A., D'Ayala, D., Sequeira, L., 2012. Assessment of wind-driven rain impact, related surface erosion and surface strength reduction of historic building materials. Build. Environ. 57, 336–348. https://doi.org/10.1016/j.buildenv.2012.05.004.

Fatorić, S., Seekamp, E., 2017. Are cultural heritage and resources threatened by climate change? A systematic literature review. Clim. Change 142 (1), 227–254. https://doi.org/10.1007/s10584-017-1929-9.

C. I. for Buildings Services Engineers, 2017. Test reference years [cited 6 September 2017]. www.cibse.org.

Ge, H., Chiu, V., Stathopoulos, T., 2017. Effect of overhang on wind-driven rain wetting of facades on a mid-rise building: field measurements. Build. Environ. 118, 234–250.

Ge, H., Chiu, V., Stathopoulos, T., Souri, F., 2018. Improved assessment of wind-driven rain on building façade based on iso standard with high-resolution on-site weather data. J. Wind Eng. Ind. Aerodyn. 176, 183–196. https://doi.org/10.1016/j.jweia.2018.03.013.

Hall, C., Hamilton, A., Hoff, W.D., Viles, H.A., Eklund, J.A., 2011. Moisture dynamics in walls: response to micro-environment and climate change. Proc. R. Soc. A Math. Phys. Eng. Sci. 467 (2125), 194–211. https://doi.org/10.1098/rspa.2010.0131.

Hall, K., 1999. The role of thermal stress fatigue in the breakdown of rock in cold regions. Geomorphology 31 (1-4), 47–63.

Hansen, J., Sato, M., 2016. Regional climate change and national responsibilities. Environ. Res. Lett. 11 (3), 034009.

Scotland, Historic Environment, 2018. A Climate Change Risk Assessment. Research and Study Report, Historic Environment Scotland.

Holmes, C., 2015. Future Changes in Wind and Rain and the Implications for Wind Driven Rain. Tech. rep., ClimateXChange.

IPCC, Stocker, T., Qin, D., Plattner, G.-K., Tignor, M., Allen, S., Boschung, J., Nauels, A., Xia, Y., Bex, V., Midgley, P. (Eds.), 2013. Summary for policymakers. Climate Change 2013: The Physical Science Basis. Contribution of Working Group I to the Fifth Assessment Report of the Intergovernmental Panel on Climate Change. Cambridge University Press., pp. 3–32. www.cambridge.org/9781107661820.

ISO, 2009. ISO 15927-3: 2009: Hygrothermal Performance of Buildings - Calculation and Presentation of Climatic Data - Part 3: Calculation of a Driving Rain Index for Vertical Surfaces From Hourly Wind and Rain Data, Standard. International Standards Organisation.

Jenkins, G.J., 2007. The Climate of the United Kingdom and Recent Trends. Met Office Hadley Centre, Exeter, England.

Jones, P., Kilsby, C., Harpham, C., Glenis, V., Burton, A., 2009. UK Climate Projections Science Report: Projections of Future Daily Climate for the UK From the Weather Generator. University of Newcastle.

Kubilay, A., Derome, D., Blocken, B., Carmeliet, J., 2015. Wind-driven rain on two parallel wide buildings: field measurements and cfd simulations. J. Wind Eng. Ind. Aerodyn. 146, 11–28.

Künzel, H.M., Kiessl, K., 1996. Calculation of heat and moisture transfer in exposed building components. Int. J. Heat Mass Transf. 40 (1), 159–167. https://doi.org/10.1016/S0017-9310(96)00084-1.

Lacy, R.E., 1951. Observations with a directional raingauge. Q. J. R. Meteorol. Soc. 77 (332), 283–292. https://doi.org/10.1002/qj.49707733213.

Laycock, E.A., Wood, C., 2014. Understanding and controlling the ingress of driven rain through exposed, solid wall masonry structures. Geol. Soc. Lond., Spec. Publ. 391 (1), 175–191.

May, N., Sanders, C.H., 2017. Moisture in Buildings: An Integrated Approach to Risk Assessment and Guidance. White Paper, BSI Group.

McCabe, S., Brimblecombe, P., Smith, B.J., McAllister, D., Srinivasan, S., Basheer, P.A.M., 2013. The use and meanings of 'time of wetness' in understanding building stone decay. Q. J. Eng. Geol. Hydrogeol. 46 (4), 469–476. https://doi.org/10.1144/qjegh2012-048.

Murphy, J.M., Sexton, D., Jenkins, G., Booth, B., Brown, C., Clark, R., Collins, M., Harris, G., Kendon, E., Betts, R., et al. 2009. UK Climate Projections Science Report: Climate Change Projections. Tech. rep., Met Office Hadley Centre.

Mylona, A., 2012. The use of UKCP09 to produce weather files for building simulation. Build. Serv. Eng. Res. Technol. 33 (1), 51–62.

Nakićenović, N., Swart, R., 2000. Special report on emissions scenarios (sres). A Special Report of Working Group III of the Intergovernmental Panel on Climate Change, IPCC, Geneva.

NCAS British Atmospheric Data Centre, 2012, 5 September 2017. Met Office Integrated Data Archive System (MIDAS) Land and Marine Surface Stations Data (1853-current). URL http://catalogue.ceda.ac.uk/uuid/220a65615218d5c9cc9e4785a3234bd0.

Nik, V., Sasic Kalagasidis, A., 2014. Wind driven rain and climate change: A simple approach for the impact assessment and uncertainty analysis. Proceedings of 10th Nordic Symposium on Building Physics. pp. 574–581.

Nik, V.M., 2017. Application of typical and extreme weather data sets in the hygrothermal simulation of building components for future climate - a case study for a wooden frame wall. Energ. Buildings 154, 30–45. https://doi.org/10.1016/j.enbuild.2017.08.042.

Nik, V.M., Mundt-Petersen, S., Kalagasidis, A.S., Wilde, P.D., 2015. Future moisture loads for building facades in Sweden: climate change and wind-driven rain. Build. Environ. 93, 362–375. https://doi.org/10.1016/j.buildenv.2015.07.012.

Pakkala, T.A., Lemberg, A.-M., Lahdensivu, J., Pentti, M., 2016. Climate change effect on wind-driven rain on facades. Nordic Concrete 31, 31–49.

Peel, M.C., Finlayson, B.L., McMahon, T.A., 2007. Updated world map of the köppen-geiger climate classification. Hydrol. Earth Syst. Sci. 11 (5), 1633–1644. https://doi.org/10.5194/hess-11-1633-2007.

Pérez-Bella, J.M., Domínguez-Hernández, J., Rodríguez-Soria, B., del Coz-Díaz, J.J., Cano-Suñén, E., 2012. Estimation of the exposure of buildings to driving rain in Spain from daily wind and rain data. Build. Environ. 57, 259–270.

Pérez-Bella, J.M., Domínguez-Hernández, J., Rodríguez-Soria, B., del Coz-Díaz, J.J., Cano-Suñén, E., 2013. Combined use of wind-driven rain and wind pressure to define water penetration risk into building façades: the Spanish case. Build. Environ. 64, 46–56.

Pettersson, K., Krajnovic, S., Kalagasidis, A., Johansson, P., 2016. Simulating wind-driven rain on building facades using Eulerian multiphase with rain phase turbulence model. Build. Environ. 106, 1–9. https://doi.org/10.1016/j.buildenv.2016.06.012.

Prior, J., 1985. Directional Driving Rain Indices for the United Kingdom: Computation and Mapping (Background to BSI Draft for Development DD93). Building Research Establishment.

Prior, M.J., 1983. Improved (directional) driving rain indices for the United Kingdom - computation, mapping and applications. Symposium on building climatology, September 20-24, 1982, Moscow. Proceedings, Part III.. pp. 187–199. International Council for Building Research, Studies and Documentation (CIB).

Reid, J., Garvin, S., 2011. Wind Driven Rain: Assessment of the Need for New Guidance. Tech. Rep. A1533015, Building Research Establishment Scotland.

Smith, B.J., McCabe, S., McAllister, D., Adamson, C., Viles, H.A., Curran, J.M., 2011. A commentary on climate change, stone decay dynamics and the 'greening' of natural stone buildings: new perspectives on 'deep wetting'. Environ. Earth Sci. 63 (7), 1691–1700. https://doi.org/10.1007/s12665-010-0766-1.

Stelfox, D., 2018. Personal Correspondence., Interview. 1 February.

Straube, J., Burnett, E., 2000. Simplified prediction of driving rain on buildings. Proc. of the International Building Physics Conference. Eindhoven., pp. 375–382.

Straube, J.F., Burnett, E.F., 1998. Driving rain and masonry veneer. Water leakage through building facades. Vol. Special Technical Publication, ASTM STP 1314. ASTM International, pp. 73–87.

Tang, W., Davidson, C.I., Finger, S., Vance, K., 2004. Erosion of limestone building surfaces caused by wind-driven rain: 1. Field measurements. Atmos. Environ. 38 (33), 5589–5599.

UK Climate Projections, Weather generator [online] (March 2012) [cited 20 September 2017].

Underwood, J.S., Meentemeyer, V., 1998. Climatology of wind-driven rain for the contiguous United States for the period 1971–1995. Phys. Geogr. 19 (6), 445–462. https://doi.org/10.1080/02723646.1998.10642661.

Warscheid, T., Braams, J., 2000. Biodeterioration of stone: a review. Int. Biodeterior. Biodegrad. 46 (4), 343–368.

Watkins, R., Levermore, G., Parkinson, J., 2011. Constructing a future weather file for use in building simulation using UKCP09 projections. Build. Serv. Eng. Res. Technol. 32 (3), 293–299.

Watts, G., Battarbee, R.W., Bloomfield, J.P., Crossman, J., Daccache, A., Durance, I., Elliott, J.A., Garner, G., Hannaford, J., Hannah, D.M., et al. 2015. Climate change and water in the UK-past changes and future prospects. Prog. Phys. Geogr. 39 (1), 6–28.

Wilks, D.S., Wilby, R.L., 1999. The weather generation game: a review of stochastic weather models. Prog. Phys. Geogr. 23 (3), 329–357. https://doi.org/10.1177/030913339902300302.